Systemic risk measured by the resiliency of the system to initial shocks

Klinčić, Luka; Zlatić, Vinko; Caldarelli, Guido; Štefančić, Hrvoje

Systemic risk measured by the resiliency of the system to initial shocks

Luka Klinčić,[1] Vinko Zlatić,[2] Guido Caldarelli,[3,4,5,6,7] and Hrvoje Štefančić[8]
[1]*Department of Physics, Faculty of Science, University of Zagreb, Bijenička c. 32, 10000 Zagreb, Croatia*
[2]*Theoretical Physics Division, Rudjer Bošković Institute, Bijenička c. 54, 10000 Zagreb, Croatia*
[3]*DMSN, Ca' Foscari University of Venice, Via Torino 155, 30172 Venice, Italy*
[4]*European Centre for Living Technology (ECLT), Dorsoduro 3911, 30123 Venice, Italy*
[5]*Institute for Complex Systems (ISC), CNR, UoS Sapienza, Piazzale Aldo Moro 2, 00185 Rome, Italy*
[6]*London Institute for Mathematical Sciences (LIMS), W1K2XF London, United Kingdom*
[7]*Fondazione per ilFuturo delle Città (FFC), Via Boccaccio 50, 50133 Firenze, Italy*
[8]*Catholic University of Croatia, Ilica 242, 10000 Zagreb, Croatia*

(Received 14 April 2023; accepted 13 September 2023; published 5 October 2023)

The analysis of systemic risk often revolves around examining various measures utilized by practitioners and policymakers. These measures typically focus on assessing the extent to which external events can impact a financial system, without delving into the nature of the initial shock. In contrast, our approach takes a symmetrical standpoint and introduces a set of measures centered on the quantity of external shock that the system can absorb before experiencing deterioration. To achieve this, we employ a linearized version of DebtRank, which facilitates a clear depiction of the onset of financial distress, thereby enabling accurate estimation of systemic risk. Through the utilization of spectral graph theory, we explicitly compute localized and uniform exogenous shocks, elucidating their behavior. Additionally, we expand the analysis to encompass heterogeneous shocks, necessitating computation via Monte Carlo simulations. We firmly believe that our approach is both comprehensive and intuitive, enabling a standardized assessment of failure risk in financial systems.

DOI: 10.1103/PhysRevE.108.044303

I. INTRODUCTION

The investigation of networks in natural and social systems has yielded numerous intriguing models that aim to elucidate both their topology and the dynamics occurring within them [1]. Among these dynamic models, a significant and wide-ranging focus lies in understanding the systemic breakdown of such systems. Particularly, a notable area of interest within this category of models is the examination of systemic risk in economics, specifically within financial systems [2–5].

Systemic risk, which pertains to the risk of widespread collapse within a complex system, has become a substantial concern for scholars and a vital issue for policymakers and regulators. One approach to analyzing and comprehending systemic risk involves the utilization of complexity theory and network analysis [6]. These methodologies enable the exploration of interconnections and dependencies among financial institutions [7]. Research has demonstrated that the network structure of the financial system plays a significant role in the transmission of shocks and the likelihood of contagion. For instance, a recent study [8] has illustrated how a network model can be employed to quantify and manage systemic risk in the interbank market, also known as the "interbank network." Likewise, it has been reported [9] that a densely interconnected financial system is associated with a heightened level of systemic risk.

This intuition resulted in more quantitative analysis on specific cases of interest [10–13]. Recent research on systemic risk extends the financial network to multilayer networks, including different assets and types of loans, etc. [14–16]. These studies have provided some of the first evidence about the importance of network analysis in understanding and mitigating systemic risk and have been applied to inform regulators [10], in order to individually assess a systemic risk [17], to simulate different policies, such as bank taxation [18,19], or to understand which network architectures are more and which are less risky [20].

Another important aspect of analyzing systemic risk is the use of debt ranking [10]. Debt ranking is a technique used to assign a relative importance or "rank" to various financial institutions, taking into account their level of debt and their position within the network. Similar to other centrality measures, debt ranking enables the identification of the most systemically significant institutions, commonly known as "too-big-to-fail" or "too-connected-to-fail" institutions. These institutions are regarded as crucial for maintaining the stability of the financial system and consequently face more stringent regulations and oversight.

The significance of the networked structure of the financial system in comprehending systemic risk has garnered substantial attention in economic literature. One of the pioneering works addressing this subject [21] examines the influence of factors such as capitalization levels, bank connectivity, interbank exposures, system concentration, liquidity, and the tier structure of the financial system on systemic risk. A recent notable review of the economic literature on systemic risk in financial networks can be found in [22]. In their work, the authors classify systemic risks in financial networks into two categories: "contagion through direct externalities" and "various feedback effects that permit multiple equilibria and

self-fulfilling prophecies." The approach taken in this paper is appropriate to study the first type of systemic risks and builds on a number of papers introduced in economic literature, such as [23–25], to name a few.

The aforementioned measures of systemic risk in networked systems are all derived from the impact on the financial system following a systemic event and the subsequent propagation of default cascades throughout the financial network [26].

In this paper, we introduce an approach to quantifying systemic risk, focusing on the "amount of external shock the system can withstand before experiencing a systemic event." We define a systemic event as the default of a financial institution resulting from the propagation of shocks through the network. From a technical perspective, the measurement of systemic risk involves solving an inverse problem and estimating the initial conditions leading to systemic events in the models. While this approach may appear more complex compared to conventional methods, we demonstrate its efficacy through a networked systemic risk model, i.e., the DebtRank [27]. By adopting this approach, we can gain valuable insights into the phenomenon and develop quantitative measures that extend risk analysis to encompass all potential scenarios of exogenous shocks. This broader perspective allows for a more comprehensive understanding of systemic risk and facilitates the provision of generalized quantitative measures.

Section II of our paper introduces the version of DebtRank utilized in our analysis and elucidates its suitability for addressing the inverse problem. We provide a comprehensive explanation of why this model is well suited for our research objectives. Moving on to Sec. III, we outline and describe three distinct types of shocks: Uniform, localized, and heterogeneous shocks. We demonstrate how each of these shocks can be evaluated using our proposed method and subsequently develop three measures of systemic risk based on these shock scenarios. In Sec. IV, we present the results obtained from our analysis. Initially, we present analytical findings based on very small networks, providing valuable insights at a microlevel. Subsequently, we present simulated results for larger networks, offering a macrolevel perspective on systemic risk dynamics. Finally, in the conclusion, we summarize our findings and discuss the implications. We also outline potential directions for further research, highlighting areas that warrant deeper exploration in the context of systemic risk analysis.

II. DEBTRANK MEASURE OF SYSTEMIC RISK

To initiate this analysis, we will begin by assuming complete knowledge of bank balances and interbank loans. The bank balance is comprised of assets (A), liabilities (L), and equity (E), and their relationship is defined by a standard balance sheet equation:

$$A = L + E. \tag{1}$$

The systemic risk in this analysis will be modeled using the DebtRank algorithm [10], specifically the version described in [27]. In this version, the financial system consists of n banks, represented as vertices in the network. The primary mode of interaction between banks is through interbank loans, which are represented as weighted edges A_{ij} in the network. The weights of these edges indicate the sum of loans that Bank i has lent to Bank j.

The total network assets of Bank i, which represents the amount of lending to other banks, is denoted as A_i and computed as $A_i = \sum_j A_{ij}$. The remaining assets of Bank i not involved in the interbank system are denoted as A_i^E. Each loan A_{ij} extended by Bank i is matched by a corresponding liability L_{ij} of Bank j, which must be repaid in the future. Liabilities of Bank i not related to the interbank financial system are denoted as L_i^E. The equity of Bank i is calculated using the above defined balance sheet equation (1): $E_i = A_i - L_i$

In this paper, we define a bank i as bankrupt if its liabilities exceed its assets, i.e., when $E_i \leqslant 0$. To analyze the evolution of the system, we consider the set of nonbankrupted banks at time t

$$\mathcal{A}(t) = \{j : E_j(t) > 0\}. \tag{2}$$

A further assumption is that when the bank j goes bankrupt, its assets are taken from the system, i.e., $A_{ij} = 0$, but liabilities remain L_{ij} constant. This leads to the temporal balance equation

$$E_i(t) = A_i^E(t) - L_i^E(t) + \sum_{j\in\mathcal{A}(t-1)} A_{ij}(t) - \sum_{j=1}^{n} L_{ij}(t), \tag{3}$$

in which the sum of assets includes only the banks that were "healthy" at time $t-1$, i.e., we assume that the information of bankruptcy takes one unit of time.

This leads to the following mechanism of the propagation of financial shock, under the assumption that the assets of the lender are changed proportionally to the equity of the borrower in the previous time stamp, i.e.,

$$A_{ij}(t+1) = \begin{cases} A_{ij}(t)\frac{E_j(t)}{E_j(t-1)}, & j \in \mathcal{A}(t-1), \\ A_{ij}(t) = 0, & j \notin \mathcal{A}(t-1). \end{cases} \tag{4}$$

Time evolution of assets can be computed using Eqs. (3) and (4) to get

$$E_i(t+1) - E_i(t) = \sum_{j\in\mathcal{A}(t-1)} \frac{A_{ij}(0)}{E_j(0)}(E_j(t) - E_j(t-1)), \tag{5}$$

where Eq. (3) was used recursively, and $A_{ij}(1) = A_{ij}(0)$.

The evolution of equity can be written as

$$E_i(t+1) = \max\left[0,\ E_i(t) + \sum_{j=1}^{n} \tilde{\Lambda}_{ij}(t)(E_j(t) - E_j(t-1))\right], \tag{6}$$

in which

$$\tilde{\Lambda}_{ij}(t) = \begin{cases} \frac{A_{ij}(0)}{E_j(0)}, & j \in \mathcal{A}(t-1), \\ 0, & j \notin \mathcal{A}(t-1). \end{cases} \tag{7}$$

Here the maximum ensures that the equity after the bankruptcy cannot become negative. Now we define financial shock on bank i as

$$h_i(t) = \frac{E_i(0) - E_i(t)}{E_i(0)} \tag{8}$$

and using also (7) the evolution of financial shock is

$$h_i(t+1) = \min\left[0, h_i(t) + \sum_{j=1}^{n} \Lambda_{ij}(t)(h_j(t) - h_j(t-1))\right]. \tag{9}$$

A key component of DebtRank dynamics is the fact that the system stability is completely determined by the properties of matrix $\Lambda(t)$.

We consider the time period between two bankruptcies, i.e., a period in which the matrix $\Lambda(t) = \Lambda$ is constant. Defining the change of financial shock as $\Delta h(t) = h(t) - h(t-1)$ and using the fact that $h(0) = 0$, Eq. (9) can be written in a matrix form

$$\begin{aligned}\Delta h(t+1) &= \Lambda \Delta h(t) \\ &= \Lambda^t \Delta h(1) = \Lambda^t h(1).\end{aligned} \tag{10}$$

The financial shock at $t+1$ is a sum of previous shocks

$$h(t+1) = \sum_{t'=1}^{t+1} \Delta h(t') = \sum_{t'=0}^{t} \Lambda^{t'} h(1). \tag{11}$$

The asymptotic value of shocks $h^\infty = \lim_{t\to\infty} h(t)$ is finite if $\|\Lambda\| < 1$. Gelfand theorem states that the spectral radius $\rho(\Lambda) = \max_{1\leqslant i\leqslant n}(\lambda_i)$ can for a square matrix always be written as

$$\rho(\Lambda) = \lim_{k\to\infty} \|\Lambda^k\|^{\frac{1}{k}}. \tag{12}$$

If the spectral radius is smaller than 1, i.e., $|\lambda_{max}| < 1$, the asymptotic value of financial shock converges towards

$$h^\infty = (I - \Lambda)^{-1} h(1)\,. \tag{13}$$

In the opposite case $|\lambda_{max}| \geqslant 1$, the initial financial shock consumes the whole system.

It is, in principle, possible to simulate the propagation of shocks such that when an institution goes bankrupt the matrix Λ reduces its rank, but in the following we will focus our attention only on constant matrices Λ.

III. CONDITIONS ON INITIAL SHOCKS FOR BANKRUPTCY-FREE RISK PROPAGATION

The primary scientific inquiry addressed in this paper is the following: Which initial shocks result in systemic effects within the financial system? Considering the vast number of potential configurations of initial shocks capable of destabilizing the financial system, which increases exponentially with the system's size, we strive to ensure the coherency of our analysis by focusing on three distinct types of shocks. The first type of shock we examine is the uniform shock, representing a significant exogenous event that impacts all institutions within the system equally, resulting in a uniform fraction of asset loss for each institution. The second type is a localized shock, which involves a shock solely affecting a single institution within the system, while the others remain unaffected. Lastly, we investigate a more comprehensive scenario by combining the previous two types of shocks. This multiparametric shock affects all institutions, but with varying intensities. We quantify the intensity of this mixed shock using the associated hypervolume, as we will elaborate upon in subsequent discussions.

A. Uniform shock

Uniform shock represents one of the most common macroeconomic shocks that can arise from various causes. It can be associated with demand and supply fluctuations, changes in legislation affecting financial markets, inflation, and other factors. Financial systems are vulnerable to external conditions and are influenced by global events that often uniformly impact similar firms. While financial systems are designed to be relatively resilient to such events, significant uniform shocks can lead to substantial problems for these systems.

To model the uniform shock, we employ Eq. (13). In this case, we set the same initial value, denoted as $h(1)$, for all components of the vector. Specifically, for each component i, we have $h_i(1) = \psi_u$. This allows us to express the uniform shock as follows:

$$h(1) = \psi_u \begin{pmatrix} 1 \\ 1 \\ \vdots \\ 1 \end{pmatrix} = \psi_u \widetilde{h(1)}. \tag{14}$$

If the uniform shock is used in Eq. (13)

$$h^\infty = \psi_u (I - \Lambda)^{-1} \widetilde{h(1)}. \tag{15}$$

We denote as Ψ_u the maximal uniform shock that the system can absorb. To compute it, we need to maximize Eq. (15):

$$\Psi_u = \frac{1}{\max_j[((I - \Lambda)^{-1}\widetilde{h(1)})_j]}. \tag{16}$$

The Ψ_u depends only on the details of the network, i.e., on the amounts of interbank assets and leverage of the banks. Larger values of Ψ_u are associated with larger shocks the system can tolerate and therefore to a larger resilience of the system. Conversely, smaller values of Ψ_u indicate systems more susceptible to the exogenous uniform risks.

B. Localized shock

In contrast to the uniform shock, the localized shock represents the extreme end of the spectrum of potential shocks. It specifically models financial difficulties that arise within a single financial institution. However, what sets the localized shock apart is that the affected institution is systemically important, meaning that its default has the potential to trigger instability within the entire financial system.

Localized shocks have historically exerted a significant impact on modern financial systems. A notable example is the default of Lehman Brothers in 2008, which acted as a triggering event for the global financial crisis. At the time, Lehman Brothers was the fourth-largest investment bank in the United States. Its default resulted in the propagation of financial shocks to its counterparties, contributing significantly to the largest decline in the Dow Jones index in recorded history [28].

The measure of systemic risk from uniform shock is developed in a similar way as measures of uniform shock by using

Eq. (13). The vector of initial shock $h_i(1)$ is the ith unitary vector $\boldsymbol{e}_i$ multiplied by ${\psi_l}^i$

$$h(1)^i = {\psi_l}^i \begin{pmatrix} 0 \\ \vdots \\ 1 \\ \vdots \\ 0 \end{pmatrix} = {\psi_l}^i \boldsymbol{e}_i. \tag{17}$$

Considering a network of n banks, there are n different initial conditions for localized shock, each of them representing the problem in the bank it represents. We are interested in maximal ${\psi_l}^i$ for which some element of $(h^\infty)^i$ becomes 1,

$$\begin{aligned}(h^\infty)^i_j &= {\psi_l}^i((I-\Lambda)^{-1}\boldsymbol{e}_i)_j \\ &= {\psi_l}^i \sum_{k=1}^{n}((I-\Lambda)^{-1})_{jk}\delta_{ki} = {\psi_l}^i((I-\Lambda)^{-1})_{ji},\end{aligned} \tag{18}$$

where δ_{ki} is the Kronecker delta. We define *maximal allowed localized shock* (MALS) as a value of local shock that maximizes Eq. (18)

$${\Psi_l}^i = \frac{1}{\max_j[((I-\Lambda)^{-1})_{ji}]}. \tag{19}$$

The value of ${\Psi_l}^i$ is solely determined by the reduced adjacency matrix Λ, specifically relying on a single element of the inverse matrix $(I-\Lambda)^{-1}$. This measure can be interpreted as an assessment of the resilience of individual institutions in initiating a financial bankruptcy cascade. Rather than considering a single numerical value, we can shift our attention to the individual components of the vector Ψ_l. This approach provides a comprehensive overview of the maximum absolute localized shock (MALS) for different elements within the network.

Within this context, an important measure that we introduce is the minimal component of the maximally defined localized shock,

$$\Psi_l^m = \min_i \Psi_l^i, \tag{20}$$

which signifies the largest allowed localized shock to any institution that can be sustained by the least resilient constituent of the system.

C. Heterogenous financial shock

Uniform and localized financial shocks represent two extreme scenarios that can result in systemic risk within the considered financial system. Both cases can be characterized by a single parameter ψ, which serves as a metric to evaluate the risk level of the system. Scalar measures like this are valuable to both researchers and practitioners as they simplify the assessment of the system to a single quantifiable value.

However, the applicability of these scalar measures can be questioned in real-world situations where multiple different shocks may occur simultaneously within the financial system. In such cases, the system consists of n financial institutions, each potentially experiencing a distinct parameter of financial shock. It becomes relevant to explore various combinations of initial shocks that still maintain system stability. To address this, we propose a measure associated with such a shock, which is also represented by a scalar quantity. This measure is derived from the iterative evolution of cumulative capital loss, as depicted in Eq. (13), while observing this equation as a linear transformation within the allowed subspace h^∞:

$$h(1) = (I-\Lambda)h^\infty. \tag{21}$$

Considering that the default of financial institution i occurs when $h_i^\infty = 1$, the entire subspace where no defaults occur in the system ($0 \leqslant h_i^\infty < 1$) corresponds to an n hypercube. This hypercube is situated at the origin of a coordinate space defined by the axes h_i^∞. Consequently, all the admissible scenarios in which no financial institution suffers damage are confined within this hypercube.

In order to determine the values of the subspace of initial shock parameters $h(1)$ that correspond to a default-free system, we perform a transformation from the space of asymptotic shock to the subspace of initial shock using Eq. (21).

The matrix Λ contains non-negative elements, with the diagonal elements always equal to zero, indicating that institutions do not invest in themselves. As a result, the general form of the matrix $I-\Lambda$ has 1's on the diagonal and all other elements are nonpositive:

$$I-\Lambda = \begin{pmatrix} 1 & -\Lambda_{12} & \dots & -\Lambda_{1n} \\ -\Lambda_{21} & 1 & & \vdots \\ \vdots & & \ddots & \\ -\Lambda_{n1} & \dots & & 1 \end{pmatrix}. \tag{22}$$

Regarding the linear transformation of the hypercube, it implies that the subspace of initial shock parameters, denoted as $h(1)$, will necessarily encompass values outside the strictly positive 2^n-tant. In other words, the values of $h(1)_i$ that correspond to a default-free system may include values outside the realistic interval of $[0, 1\rangle$. These values should be disregarded as they represent positive initial shocks, indicating an increase in institutional assets. Consequently, the relevant subspace of interest, denoted as V, is the intersection of the allowed subspace of $h(1)$ and the positive 2^n-tant.

Depending on the matrix Λ the subspace of allowed initial shocks can be larger or smaller. In other words, if the network structure is such that the subspace of initial shocks V is small, and we know that all the other combinations of initial shock lead to the default of at least one institution, then this network structure is of low resiliency. On the other hand, if V is of a size similar to the size of the subspace h^∞, the probability that the initial combination of shocks will lead to default is small.

Therefore, it makes sense to measure the risk of the system in terms of *hypervolume* Ψ_V of allowed subspace V. If the intersection with 2^n-tant were not important, the computation of this measure would trivially be $\det(I-\Lambda)$. Unfortunately, depending on the sum of interbanks investments, the geometry of the problem can be extremely complex even for a small number of vertices.

In order to demonstrate the complexity and provide some intuition of analytical analysis we perform exact computations on a few small networks.

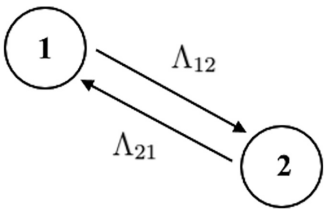

FIG. 1. Network of $n = 2$ vertices with mutual exposures.

IV. RESULTS

A. Network of $n = 2$ vertices

The simplest possible network of interest is the network of two institutions, creating the $n = 2$ network as represented in Fig. 1.

In that case the matrix of transformation is

$$I - \Lambda = \begin{pmatrix} 1 & -\Lambda_{12} \\ -\Lambda_{21} & 1 \end{pmatrix}, \tag{23}$$

while its inverse is

$$(I - \Lambda)^{-1} = \frac{1}{1 - \Lambda_{12}\Lambda_{21}} \begin{pmatrix} 1 & \Lambda_{12} \\ \Lambda_{21} & 1 \end{pmatrix}. \tag{24}$$

We can easily compute measures of uniform and localized shock as

$$\Psi_u = \frac{1 - \Lambda_{12}\Lambda_{21}}{1 + \max[\Lambda_{12},\ \Lambda_{21}]}, \tag{25}$$

$$\Psi_l = (1 - \Lambda_{12}\Lambda_{21}) \begin{pmatrix} \min\left[1,\ \frac{1}{\Lambda_{21}}\right] \\ \min\left[1,\ \frac{1}{\Lambda_{12}}\right] \end{pmatrix}. \tag{26}$$

Hypervolume in this case corresponds to the surface of the parallelogram, which is computed through transformation and is confined in the first quadrant. The measure of heterogeneous shock is then

$$\Psi_V = 1 - \tfrac{1}{2}\left[\Lambda_{12}\left(1 - \Lambda_{21}^2\right) + \Lambda_{21}\left(1 - \Lambda_{12}^2\right)\right]. \tag{27}$$

Allowed intervals of initial shock that do not produce default in the system can be computed using relations $0 \leqslant h_i^{\infty} < 1$, $i \in \{1, 2\}$, which leads to

$$0 \leqslant \frac{h(1)_1 + \Lambda_{21} h(1)_2}{1 - \Lambda_{12}\Lambda_{21}} < 1,$$
$$0 \leqslant \frac{\Lambda_{12} h(1)_1 + h(1)_2}{1 - \Lambda_{12}\Lambda_{21}} < 1. \tag{28}$$

B. Network of $n = 3$ vertices

In the case of $n = 3$ there are two independent cases for which one can obtain all the other configurations through a cyclical change of indices of Λ_{ij}. We omit the cases with two edges as they are not that interesting. Two possible configurations of three vertices and three edges are presented in Fig. 2.

The set of parameters that given the evolution of financial shocks is represented by matrix $I - \Lambda$ and configuration with $n = 3$ will according to its matrix type be called upper

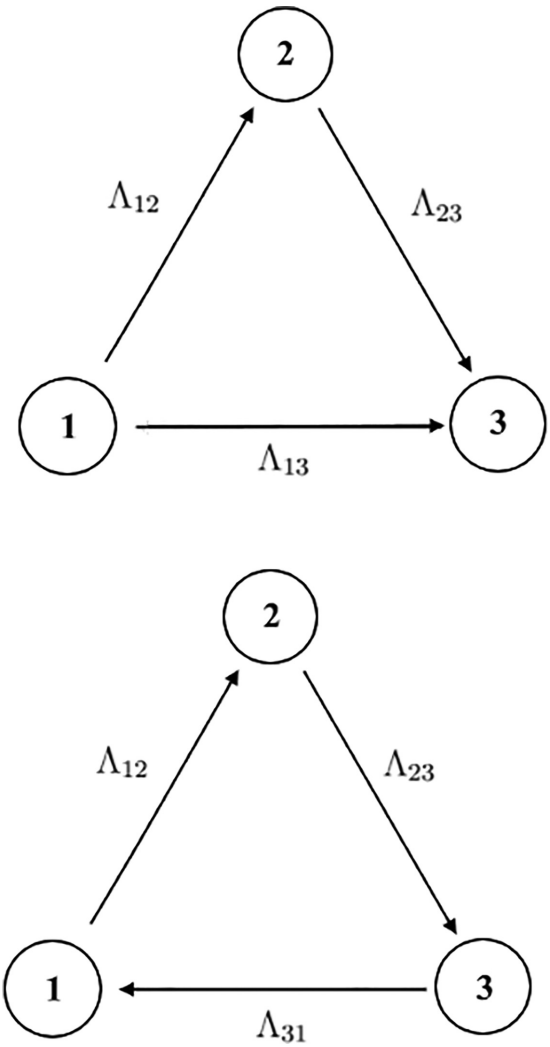

FIG. 2. In the upper panel is upper triangular and in the lower panel is a cyclical configuration of network with $n = 3$ vertices.

triangular (index UT) and cyclical (index cyc). Matrices of evolution for both cases are given by

$$I - \Lambda_{UT} = \begin{pmatrix} 1 & -\Lambda_{12} & -\Lambda_{13} \\ 0 & 1 & -\Lambda_{23} \\ 0 & 0 & 1 \end{pmatrix}, \tag{29}$$

$$I - \Lambda_{\text{cyc}} = \begin{pmatrix} 1 & -\Lambda_{12} & 0 \\ 0 & 1 & -\Lambda_{23} \\ -\Lambda_{31} & 0 & 1 \end{pmatrix}. \tag{30}$$

Inverses of $I - \Lambda$ matrices are needed for computation of measures of risk and are given by

$$(I - \Lambda_{UT})^{-1} = \begin{pmatrix} 1 & \Lambda_{12} & \Lambda_{12}\Lambda_{23} + \Lambda_{13} \\ 0 & 1 & \Lambda_{23} \\ 0 & 0 & 1 \end{pmatrix}, \tag{31}$$

$$(I - \Lambda_{\text{cyc}})^{-1} = \frac{\begin{pmatrix} 1 & \Lambda_{12} & \Lambda_{12}\Lambda_{23} \\ \Lambda_{23}\Lambda_{31} & 1 & \Lambda_{23} \\ \Lambda_{31} & \Lambda_{31}\Lambda_{12} & 1 \end{pmatrix}}{1 - \Lambda_{12}\Lambda_{23}\Lambda_{31}}. \tag{32}$$

Similar to the $n = 2$ case, maximal uniform and localized shocks are for the upper-triangular case

$$\Psi_u^{UT} = \frac{1}{1 + \max[\Lambda_{13} + \Lambda_{12}(1 + \Lambda_{23}),\ \Lambda_{23}]}, \tag{33}$$

$$\Psi_l^{UT} = \begin{pmatrix} 1 \\ \min\left[1,\ \frac{1}{\Lambda_{12}}\right] \\ \min\left[1,\ \frac{1}{\Lambda_{23}},\ \frac{1}{\Lambda_{13}+\Lambda_{12}\Lambda_{23}}\right] \end{pmatrix}, \tag{34}$$

and for the cyclical configuration

$$\Psi_u^{\text{cyc}} = \frac{1 - \Lambda_{12}\Lambda_{23}\Lambda_{31}}{1 + \max[\Lambda_{ij}(1 + \Lambda_{jk})]}, \tag{35}$$

$$\Psi_l^{\text{cyc}} = (1 - \Lambda_{12}\Lambda_{23}\Lambda_{31}) \begin{pmatrix} \min\left[1,\ \frac{1}{\Lambda_{31}},\ \frac{1}{\Lambda_{23}\Lambda_{31}}\right] \\ \min\left[1,\ \frac{1}{\Lambda_{12}},\ \frac{1}{\Lambda_{31}\Lambda_{12}}\right] \\ \min\left[1,\ \frac{1}{\Lambda_{23}},\ \frac{1}{\Lambda_{12}\Lambda_{23}}\right] \end{pmatrix}, \tag{36}$$

where in the first equation one substitutes corresponding indices i, j, k with those for the maximal value in the square bracket.

For studied configurations of the $n = 3$ network, we can again obtain intervals of allowed initial shocks using conditions $0 \leqslant h_i^{\infty} < 1$, $i \in \{1, 2, 3\}$. As in the previous case the solution is a system of equations for upper-triangular configuration

$$\begin{aligned} &0 \leqslant h(1)_1 + \Lambda_{12}h(1)_2 + (\Lambda_{13} + \Lambda_{12}\Lambda_{23})h(1)_3 < 1, \\ &0 \leqslant h(1)_2 + \Lambda_{23}h(1)_3 < 1, \end{aligned} \tag{37}$$

and for the cyclical configuration

$$\begin{aligned} 0 &\leqslant \frac{h(1)_1 + \Lambda_{12}h(1)_2 + \Lambda_{12}\Lambda_{23}h(1)_3}{1 - \Lambda_{12}\Lambda_{23}\Lambda_{31}} < 1, \\ 0 &\leqslant \frac{\Lambda_{23}\Lambda_{31}h(1)_1 + h(1)_2 + \Lambda_{23}h(1)_3}{1 - \Lambda_{12}\Lambda_{23}\Lambda_{31}} < 1, \\ 0 &\leqslant \frac{\Lambda_{31}h(1)_1 + \Lambda_{31}\Lambda_{12}h(1)_2 + h(1)_3}{1 - \Lambda_{12}\Lambda_{23}\Lambda_{31}} < 1. \end{aligned} \tag{38}$$

Hypervolume measure of heterogeneous shock Ψ_V on the network of $n = 3$ vertices corresponds to the volume of the parallelepiped in $h(1)$ space obtained through $I - \Lambda$ transform, that is, inside the first octant. Volume Ψ_V can be computed geometrically, by cutting the parallelepiped into prisms and pyramids of known volume, but already in 3D the number of such elements becomes large, as well as the number of different geometries depending on elements Λ_{ij}. For example, the equation for hypervolume associated with upper-triangular configuration is

$$\begin{aligned} \Psi_V^{UT} &= \tfrac{1}{2}\Lambda_{12}(1 - \Lambda_{23})^2 + \tfrac{1}{2}(\Lambda_{13} + \Lambda_{12}\Lambda_{23})\left(1 - \tfrac{2}{3}\Lambda_{23}\right) \\ &\quad + \tfrac{1}{6}\Lambda_{13}\Lambda_{23} + \left(1 - \Lambda_{23} + \tfrac{1}{2}\Lambda_{23}\right)(1 - \Lambda_{12} - \Lambda_{13}), \\ &\Lambda_{23} < 1,\ \Lambda_{12} + \Lambda_{13} < 1. \end{aligned} \tag{39}$$

C. Multiple vertices

Clearly, as the size of the financial system increases, the analytical methods to compute measures such as the heterogeneous shock Ψ_V become increasingly complex. To overcome this challenge, we employ Monte Carlo simulations to estimate Ψ_V.

In the h^{∞} space, we generate M random vectors with components $0 \leqslant h_i^{\infty} < 1$ from a uniform distribution. These vectors represent the allowed subspace in h^{∞} where no defaults occur in the system. It is important to note that the hypervolume of the allowed h^{∞} subspace is always equal to one.

Next, we transform these vectors from the h^{∞} space to the $h(1)$ space using Eq. (21). This transformation allows us to evaluate the initial shock conditions that lead to the absence of defaults in the system.

Within the $h(1)$ space, we determine the number of points, denoted as M', that fall within the intersection of the polytope (representing the allowed shock conditions) and the positive 2^n-tant. The 2^n-tant refers to the region where all components $h(1)_i$ are positive, representing realistic initial shock values.

Since the number of generated points is proportional to the hypervolume $\det(I - \Lambda)$ of the polytope, we estimate the volume Ψ_V of the allowed initial conditions by calculating the ratio M'/M. This provides an approximation of the hypervolume of the allowed parameter space that leads to stable financial conditions without defaults.

By employing Monte Carlo simulations and estimating Ψ_V in this manner, we can overcome the analytical complexities associated with computing measures for larger financial systems. This approach allows us to effectively assess the riskiness of different initial shock conditions and provides valuable insights into the stability of the financial system

$$\Psi_V = \frac{M'}{M} \det(I - \Lambda). \tag{40}$$

To estimate risk measures in more complex architectures, we will utilize a complete asymmetric simple digraph (CASD) and our variant of the random network model. The choice of using a CASD is motivated by the fact that many financial networks exhibit dense connections and a complete network represents the limit of high density. Additionally, complete networks reflect a highly diversified investment pattern, which is generally believed to reduce individual risk but potentially increase systemic risk.

By employing a CASD, we can capture the intricacies and interdependencies of financial institutions in a densely connected network. This allows us to analyze and evaluate the systemic risk within such complex architectures. Furthermore, our random network model variant provides an additional perspective by introducing stochastic elements that mimic real-world network structures.

Through the combination of CASD and our random network model, we aim to gain insights into the risk characteristics of financial systems operating under diverse network architectures. This analysis will help us understand how network structure and connectivity impact systemic risk, providing valuable information for risk management and policy decisions [11].

The CASD is produced by generating the matrix Λ. The algorithm used to generate CASD is explained in the following steps.

(1) We choose n vertices.

(2) We assume that the equity of all constituents is equal, i.e., $E_i = E$, and investments among the banks A_{ij} are chosen randomly from the uniform distribution on interval $[0, A]$.

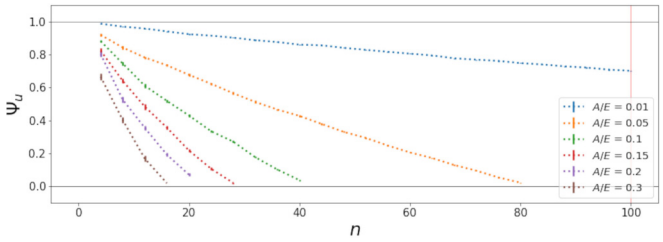

FIG. 3. On the y axis is maximal allowed uniform shock on CASD network Ψ_u; on the x axis is the size of the system n, $n \in [5, 100]$. Investigated parameters A/E are listed in the legend.

(3) For each pair of indices $i, j < n,\ i < j$ a random number drawn from uniform distribution $p' \in [0, 1]$ is generated. If $p' < 0.5$ to the element A_{ij} we assign a random value, and in the opposite case the same value is assigned to the element A_{ji}.

(4) Matrix elements A_{ij} are divided with the constant equity E leading to reduced adjacency matrix Λ.

(5) We check if the spectral radius of matrix Λ is smaller than 1; if not, we go back to step (1).

Except by parameters A and E, the incomplete random network is also described by additional parameter p giving the probability that the two randomly chosen vertices are connected with a directional edge. In order to produce this network in the above algorithm after the second step we introduce an intermediate step in which a parameter $p \in [0, 1]$ is chosen and for each pair of vertices $i, j < n,\ i < j$ we generate a random number $p'' \in [0, 1]$. If $p'' < p$, the vertices will be connected and otherwise they will not be connected. After this step, steps (3)–(5) are repeated.

1. Uniform shock Ψ_u

The measure of uniform shock, Ψ_u, is computed for the case of the CASD network. The main focus is to understand the dependence of Ψ_u on different network parameters. The simulation is performed on an ensemble of $N = 100$ networks.

First, we investigate how Ψ_u depends on the size of the network. The results are presented in Fig. 3, where error bars represent the standard deviation of simulation results, denoted as $\sigma_{\bar{\Psi}_u}$. An interesting observation is that the size of the system systematically reduces Ψ_u for all choices of other parameters. This indicates that larger systems are generally more risky than smaller ones with respect to uniform shocks. Parameter A/E is related to the speed at which Ψ_u tends to zero.

Next, we continue the computation of Ψ_u on the ensemble of incomplete random networks characterized by parameters n, p, and A/E. We first examine the dependence of Ψ_u on the parameter p. Since, for values of parameters smaller than $p_c \approx \frac{1}{n}$, networks do not possess giant components, we present results only for $p > p_c$. The dependence of Ψ_u on p is shown in Fig. 4. It is evident that increasing both parameters p and n systematically reduces the allowed maximal uniform shock for all observed parameter values. This implies that both diversification and the size of the system have a negative effect on the maximum uniform shocks that institutions can withstand before defaults occur in the system.

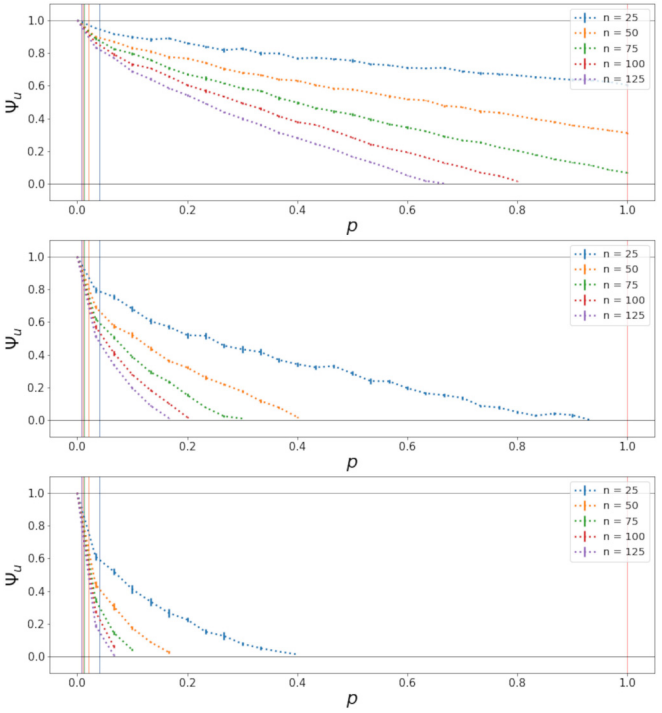

FIG. 4. Maximal allowed uniform shock on the incomplete random network. On the y axis is Ψ_u and on the x axis is the parameter of connectivity p. Sizes of networks are in the legend and are $n \in \{25, 50, 75, 100, 125\}$, while vertical lines correspond to p_c for different values of n. The top, middle, and bottom subfigures correspond to parameters A/E equal to 0.05, 0.2, and 0.5, respectively. Values of p_c are indicated by vertical colored lines.

Furthermore, in Fig. 5 for completeness, we show how the value of Ψ_u depends on A/E, although it is intuitively clear that it will get smaller with the increase of A/E.

2. Measure of localized shock Ψ_l

In the analysis related to localized financial shock, we repeat all the previous analyses but focus on the minimal component Ψ_l^m of the maximally allowed vector of localized shock Ψ_l.

Compared to the case of uniform shock, we observe a more pronounced influence of the parameter A/E on the decline of Ψ_l^m, depending on the number of vertices n. The corresponding curves now exhibit a concave shape, in contrast to the convex curves observed in the case of uniform shock. Initially, there is a period of relatively stable behavior, which becomes shorter as A/E increases. However, there is a sudden drop in the minimal value of the maximally allowed local shock. Subsequently, the measure Ψ_l^m continues to decline until it reaches a value beyond which the generated matrices Λ have a spectral radius larger than one. This signifies a critical point at which the system becomes highly susceptible to localized shocks, potentially leading to the instability of individual institutions and the overall financial system.

We again study the risk on random network varying parameters p and A/E. In this case, we used ensembles of $N = 100$ networks to have satisfactory stability of the results. Simulations are depicted in Figs. 6, 7, and 8.

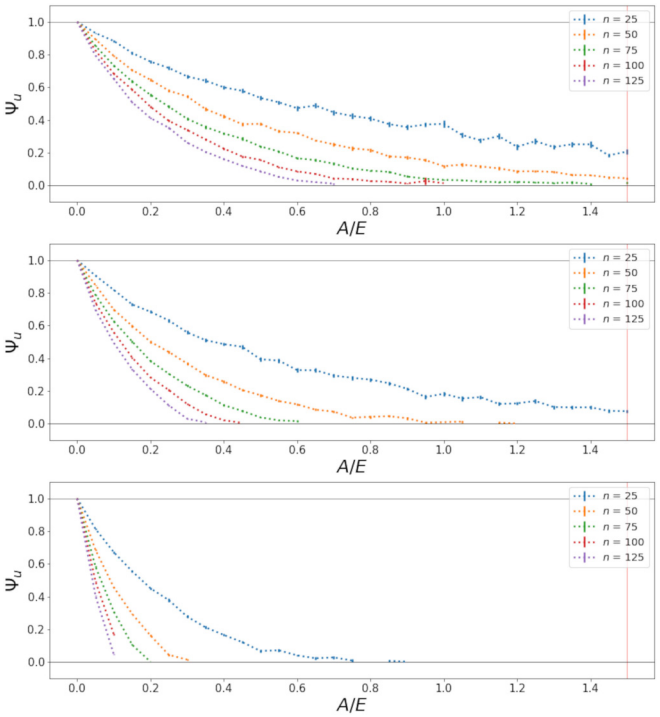

FIG. 5. Maximally allowed uniform shock of the incomplete random network depending on the parameter A/E. On the y axis is a measure Ψ_u and on the x axis is $A/E \in \langle 0, 1.5]$. Sizes of networks are in the legend and they take values $n \in \{25, 50, 75, 100, 125\}$. The top, middle, and bottom subfigures correspond to parameters p equal to 0.05, 0.1, and 0.3, respectively.

In both cases as n, p, and A/E increase the Ψ_l^m decreases monotonically. Compared to an incomplete random network this decrease is steeper for Ψ_l^m than for uniform shock Ψ_u, indicating that these parameters more strongly influence localized shocks compared to uniform ones.

An important addition to this analysis came from graph theory [29], which gives an upper bound of spectral radius $=$ $\max\{\sqrt{s_i s_o}\}$, where s_i and s_o are strengths of vertices. In our case, these values are approximately of the order A/E and are a leading contribution to this sudden collapse of the Ψ_l^m.

Up to now, we have considered the measure of localized shock Ψ_l^m, but if we want to understand more details of the distribution of risks in the network, we can take into consideration all the components of vector Ψ_l, i.e., a maximal shock with origin in any of the vertices in the network.

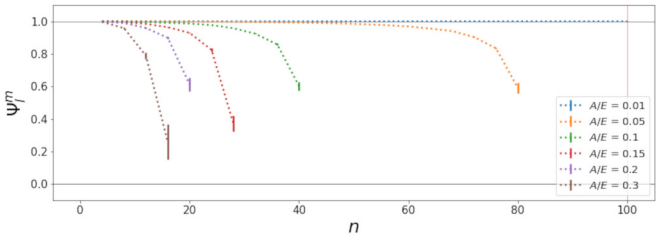

FIG. 6. Maximally allowed localized shock on CASD depending on the number of vertices. On the y axis is Ψ_l^m, while on the x axis is the size of the network $n = \in [5, 100]$. Parameter A/E is shown in the legend and it takes values $A/E \in \{0.01, 0.05, 0.1, 0.15, 0.2, 0.3\}$.

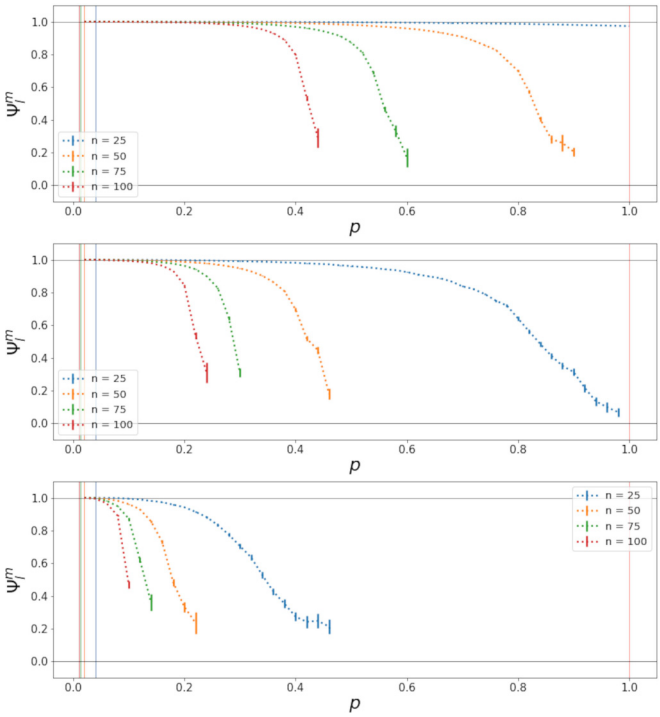

FIG. 7. Ψ_l^m on a random directed network depending on parameter p. On the y axis is Ψ_l^m, while on the x axis is $p \in \langle 0, 1]$. Network sizes $n \in \{25, 50, 75, 100\}$ are presented in the legend, while vertical lines correspond to critical values of p_c. The top, middle, and bottom subfigures correspond to parameters A/E equal to 0.1, 0.2, and 0.5, respectively.

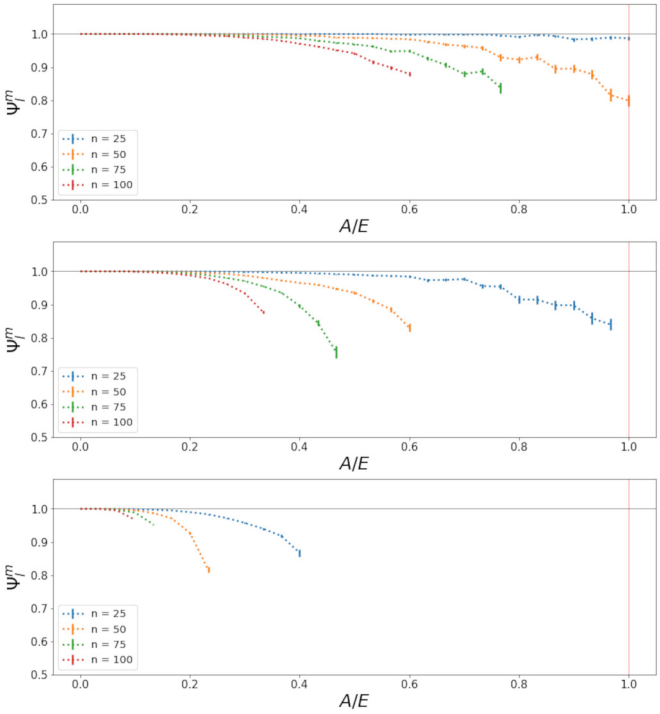

FIG. 8. Ψ_l^m on a random directed network depending on parameter A/E. On the y axis is Ψ_l^m, while on the x axis is $A/E \in \langle 0, 1]$. Network sizes $n \in \{25, 50, 75, 100\}$ are presented in the legend. The top, middle, and bottom subfigures correspond to parameters p equal to 0.05, 0.1, and 0.3, respectively.

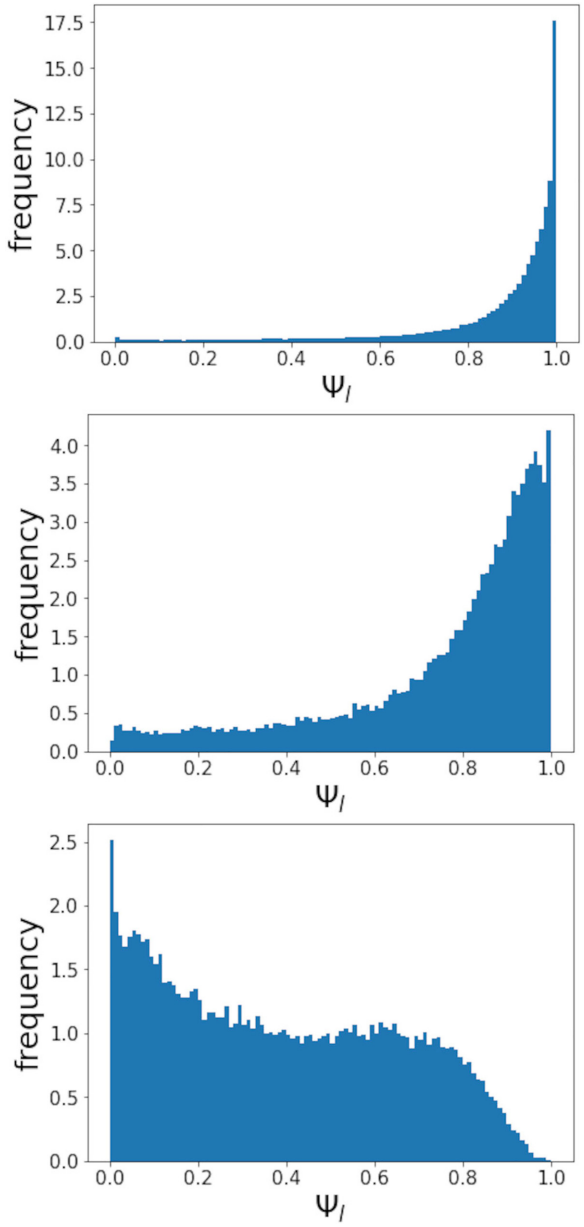

FIG. 9. Histograms of vector components of localized shock Ψ_l on the ensemble of $N = 1000$ random networks. The x axis is binned on 100 bins and the values are normalized to make the surface equal to 1. The parameters used for the top panel are $n = 75$, $p = 0.1$, and $A/E = 0.5$. The parameters used for the middle panel are $n = 50$, $p = 0.2$, and $A/E = 0.4$. The parameters used for the bottom panel are $n = 50$, $p = 0.4$, and $A/E = 0.23$.

For example, we have chosen representative parameters to represent three different states of the system. In the top panel of Fig. 9 most of the values are located around value 1, signifying the overall stability of the network. In the middle panel of Fig. 9 the distribution of values exhibits moves to the smaller values, indicating a more stressed system. In the bottom panel of Fig. 9, values are starting to cluster around $\Psi_l \approx 0$, signifying the system is close to falling apart. Such a figure can give important information about the risk of the system at a glance.

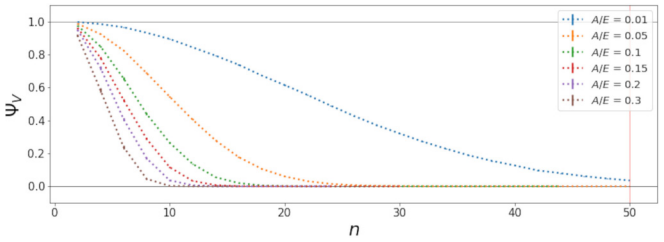

FIG. 10. Hypervolume measure Ψ_V evaluated on the CASD network depending on the number of vertices. Computation is obtained through $N = 50$ realization for each of parameters $n \in [2, 50]$ and for parameters $A/E \in \{0.01, 0.05, 0.1, 0.15, 0.2, 0.3\}$. We have used $M = 10^4$ points to evaluate hypervolume.

3. *Measure of multiparametric shock Ψ_V*

In the end, we consider the behavior of hypervolume associated shock Ψ_V dependence on network parameters. For the approximation of n-dimensional hypervolume, we use the previously described Monte Carlo method.

When comparing the results from Fig. 10 with the previous figures, we can observe that the measure Ψ_V exhibits the steepest decline with respect to n. This indicates that it evaluates the system parameters as more risky compared to the other measures.

The trend of a steeper decline in Ψ_V is also evident in Fig. 10 for an incompletely connected network. This result holds for increases in any parameter, such as n, p, or A/E, as further illustrated in Figs. 11 and 12. We believe that the reason for this behavior lies in the nature of the measure itself. The hypervolume measure Ψ_V encompasses a larger combination of initial shocks that could lead to bankruptcy, compared to the measures Ψ_u and Ψ_l. It is important to note that the hypervolume measure is inherently different from the other proposed measures, as it does not measure the allowed shock directly, but rather the relative size of the parameter space in which shocks are mitigated.

Since the hypervolume is of dimension $D = n$, equal to the number of institutions in the network, while the first two measures are 1D and represent measures along vectors spanning this hypervolume (localized shocks) or along the diagonal (uniform shocks), one might naively expect that the region protected from heterogeneous shocks scales as $\sim h^n$. As a result, the ratio of this region to the complete hypervolume becomes very small for large system size n. This could explain the more rapid decline of the hypervolume measure compared to the other measures.

It is also important to stress that the sampling of higher dimensional polytopes is a computationally expensive task if the goal is to minimize relative errors. In that sense $M = 10^4$ points would not be enough; however, (i) the goal of this research was to demonstrate the principle and (ii) we do not evaluate one polytope but we compute on an ensemble of polytopes which should in principle reduce the relative error of the algorithm.

The largest relative errors are in points where the exact hypervolume is finite but very small and the Monte Carlo measure hypervolume is zero. On the other hand, the relative error is much smaller for the more common parameter choices.

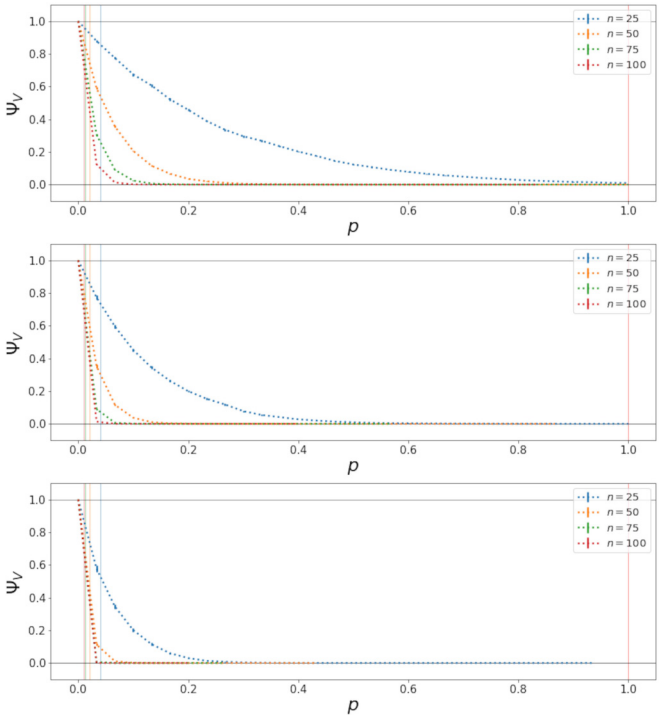

FIG. 11. Measure of hypervolume Ψ_V on a random network depending on parameter p. Computations are evaluated on the ensemble of $N = 50$ realizations for $p \in \langle 0, 1]$ and $n \in \{25, 50, 75, 100\}$. Vertical lines correspond to critical values of p_c for percolation on random networks. Figures (a), (b), and (c) correspond to parameters A/E equal to 0.05, 0.1, and 0.2. The Monte Carlo algorithm used $M = 10^4$ points.

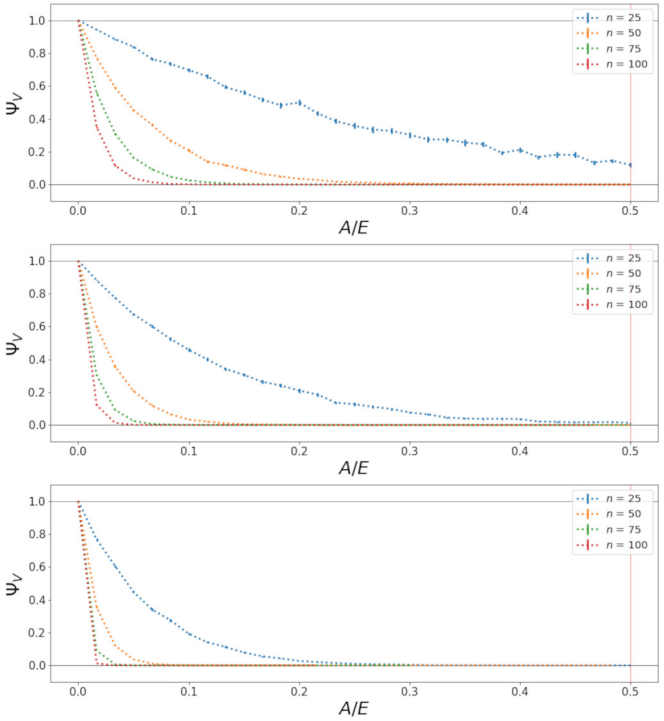

FIG. 12. Hypervolume measure Ψ_V on an incomplete random network depending on parameter A/E. Computation is carried out on an ensemble of $N = 50$ networks for $A/E \in \langle 0, 1]$ and $n \in \{25, 50, 75, 100\}$. The figures correspond to parameters p equal to 0.05, 0.1, and 0.2, respectively. The hypervolume is evaluated using $M = 10^4$ points.

This is important for practical reasons, since in the financial system a shock of small value is a common daily occurrence, while the Monte Carlo method gives better estimates for more realistic values of shock. In real systems one can use more advanced algorithms for approximation of hypervolume like *VolEsti* [30]. Another possible extension is using the historic measures of individual shocks to sample points proportionally to the expected probability of occurrence, which would better describe border cases.

4. Application to real data

To test the effectiveness of our proposed measure, as we lack data on real financial institutions, we conducted experiments using data on Croatian company defaults. The network we analyzed comprises unpaid financial obligations that resulted in court settlements. Although the data is publicly available, it is unstructured. The data set was collected as part of a project funded by the Croatian banking union and the findings were published in [31] (available in Croatian). The same network was previously utilized in [32] to assess a method for distinguishing between endogenous and exogenous default cascades in financial networks.

For our analysis, we focused on a specific subsection of the total network. In this subsection, each vertex represents a company that defaulted and every vertex has outgoing links. The network comprises 549 companies connected by 1198 edges, with a maximum degree of 60. By using this real-world data set, we aimed to evaluate the performance of our measure in a practical context.

In a study conducted in [32], it was demonstrated that financial contagion endogenously spreads in the given network. Therefore, we expect the presented measures of systemic risk to indicate a highly risky situation. While we cannot alter the structure of the network since it is predefined, we can vary the equity of companies within the network to assess its level of risk. The equity is determined by $E_i = \max(A_i, L_i) \cdot F \cdot \zeta_i$, where ζ_i is a random variable drawn from a normal distribution with a mean of 1 and a standard deviation of 0.2. The parameter F represents a multiplicative coefficient that can be adjusted and is greater than 1.

To present the results on the same plot, we introduce a scaled variant of Ψ_V, denoted as Ψ_{SV}, which is calculated as $\Psi_{SV} = \Psi_V^{1/N}$. This scaling ensures that Ψ_{SV} represents the value of a 1D uniform shock that has the same volume as the heterogenous shock. By using this scaling, we can compare and visualize the results effectively.

In Fig. 13, the measured values of the shocks are reported as a function of the multiplicative coefficient F. It is clear that the smaller uniform shock was able to start the default avalanche compared to localized shock; however, one has to keep in mind that the financial value of uniform shock spread over all the constituents was larger than any individual shock needed to start the cascade. The heterogeneous shock was hard to capture with our sampling method for values of $F < 20$, due to the size of the system. Unsurprisingly, this

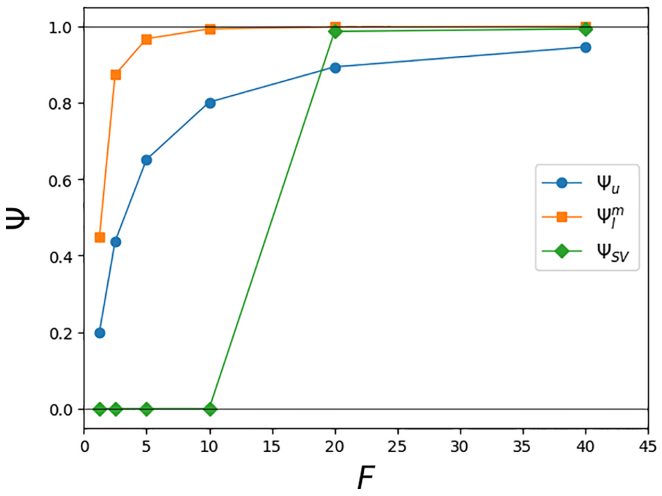

FIG. 13. Different values of shock Ψ_U (circles), Ψ_l (squares), and Ψ_{SV} (diamonds) as a function of the equity multiplication parameter F implemented on the network of Croatian defaults. Ψ_{SV} cannot be reliably computed with an ordinary sampling scheme for values of $F < 20$ due to system size.

network sample exhibits a large systemic risk for realistic values of $1 < F < 5$. Based on a historical analysis of this systemic event in Croatia, the most likely culprit was a heterogeneous shock related to the change of laws, which forced all companies to honor the maturities of their debts. This had the effect that a portion of debts companies were avoiding honoring had an immediate impact on the balance sheet of these companies. The data set is available via the link provided in [32].

V. CONCLUSIONS

This research has examined three proposed measures for systemic risk in finance. We utilized the uniform shock measure (Ψ_u) to estimate the maximum simultaneous capital decline in the system that can occur across all institutions without any of them failing. The maximally localized shock measure (Ψ_l) represents the largest shocks that an individual institution can withstand without leading to its own bankruptcy or the bankruptcy of another institution in the system. The hypervolume measure (Ψ_V) is a generalized measure that considers all intervals of initial shocks and can be approximately evaluated.

We analytically evaluated the measure equations for small networks ($n \leqslant 3$) to gain insight into the significance of different parameters. Additionally, we employed a large ensemble of random networks to evaluate the proposed measures on more realistic financial system models. Our observations yielded important findings.

First, among the presented measures, the measure of uniform shock decreases at the slowest rate with an increase in system parameters, indicating that systems are more resilient against broad, uniform external shocks. The functions for all parameter ranges appear to be concave.

Second, the measure of localized shock decreases gradually with increasing parameters until reaching a region where the system becomes highly susceptible to shocks from a single institution. For all parameter ranges, we observed that the functions seem to be convex.

Third, the hypervolume measure, which estimates heterogenous shocks, is the most conservative among the studied measures. It decreases steeply, compared to the other measures, as parameters increase. Additionally, it exhibits a combination of concave and convex regions depending on the model parameters. Since this measure is strongly sensitive to the size of the system, we also introduced a scaled measure ψ_{SV} which is 1D and more practical to compare to other measures.

The methodology explained here allows regulators to integrate conventional models for the probabilities of initial shocks with systemic risk measures in order to calculate the likelihood of systemic events within the system. An especially crucial observation for regulators pertains to the behavior of the maximum allowable localized shocks, which highlights the system's sudden vulnerability to small parameter changes. Conversely, uniform shocks demonstrate lower sensitivity to minor parameter adjustments, suggesting that regulators need to exercise relatively less caution when simulating such events.

We believe that this methodology can be of interest to regulators as it provides information on how initial shocks impact other components of the financial system, highlighting institutions whose negative behavior can significantly affect well-behaved institutions. In the future, we hope to evaluate these measures using real financial data to gain a better understanding of their behavior in a more realistic setting.

ACKNOWLEDGMENTS

H.S. and V.Z. had their research supported by the European Regional Development Fund under Grant No. KK.01.1.1.01.0009 (DATACROSS). G.C. acknowledges support from EU Project "HumanE-AI-Net," No. 952026. V.Z. wishes to acknowledge the support of the Croatian Science Foundation (HrZZ) Project No. IP-2019-4-3321 and acknowledges partial support from QuantiXLie Centre of Excellence, a Project co-financed by the Croatian Government and European Union through the European Regional Development Fund—the Competitiveness and Cohesion Operational Program (Grant No. KK.01.1.1.01.0004; element leader N.P.).

[1] M. E. Newman, A.-L. E. Barabási, and D. J. Watts, *The Structure and Dynamics of Networks* (Princeton University Press, Princeton, NJ, 2006).

[2] S. Battiston and G. Caldarelli, J. Finan. Manag. Markets Inst. **1**, 129 (2013).

[3] M. Chinazzi and G. Fagiolo, *Systemic Risk, Contagion, and Financial Networks: A Survey* (SSRN, Amsterdam, 2015).

[4] P. Gai and S. Kapadia, Oxford Rev. Econ. Policy **35**, 586 (2019).

[5] M. Bardoscia, P. Barucca, S. Battiston, F. Caccioli, G. Cimini, D. Garlaschelli, F. Saracco, T. Squartini, and G. Caldarelli, Nat. Rev. Phys. **3**, 490 (2021).
[6] S. Battiston, J. D. Farmer, A. Flache, D. Garlaschelli, A. G. Haldane, H. Heesterbeek, C. Hommes, C. Jaeger, R. May, and M. Scheffer, Science **351**, 818 (2016).
[7] G. Iori, R. Reno, G. De Masi, and G. Caldarelli, Physica A **376**, 467 (2007).
[8] P. Gai and S. Kapadia, Proc. R. Soc. A **466**, 2401 (2010).
[9] N. Beale, D. G. Rand, H. Battey, K. Croxson, R. M. May, and M. A. Nowak, Proc. Natl. Acad. Sci. USA **108**, 12647 (2011).
[10] S. Battiston, M. Puliga, R. Kaushik, P. Tasca, and G. Caldarelli, Sci. Rep. **2**, 541 (2012).
[11] S. Battiston, D. D. Gatti, M. Gallegati, B. Greenwald, and J. E. Stiglitz, J. Econ. Dyn. Control **36**, 1121 (2012).
[12] C. Minoiu and J. A. Reyes, J. Financ. Stabil. **9**, 168 (2013).
[13] M. Chinazzi, G. Fagiolo, J. A. Reyes, and S. Schiavo, J. Econ. Dyn. Control **37**, 1692 (2013).
[14] S. Battiston, G. Caldarelli, C.-P. Georg, R. May, and J. Stiglitz, Nat. Phys. **9**, 123 (2013).
[15] M. Montagna and C. Kok, ECB Working Paper No. 1944, available at SSRN: https://ssrn.com/abstract=2830546.
[16] C. D. Brummitt and T. Kobayashi, Phys. Rev. E **91**, 062813 (2015).
[17] S. Poledna, A. Hinteregger, and S. Thurner, Entropy **20**, 792 (2018).
[18] V. Zlatić, G. Gabbi, and H. Abraham, PLoS ONE **10**, e0114928 (2015).
[19] S. Poledna and S. Thurner, Quant. Financ. **16**, 1599 (2016).
[20] S. M. Krause, H. Štefančić, G. Caldarelli, and V. Zlatić, Phys. Rev. E **103**, 042304 (2021).
[21] E. Nier, J. Yang, T. Yorulmazer, and A. Alentorn, J. Econ. Dyn. Control **31**, 2033 (2007).
[22] M. O. Jackson and A. Pernoud, Annu. Rev. Econ. **13**, 171 (2021).
[23] F. Allen and D. M. Gale, An introduction to financial crises, *Wharton Financial Institutions Center Working Paper*, 2007.
[24] L. Eisenberg and T. H. Noe, Manag. Sci. **47**, 236 (2001).
[25] M. Elliott, B. Golub, and M. O. Jackson, Am. Econ. Rev. **104**, 3115 (2014).
[26] T. Roukny, H. Bersini, H. Pirotte, G. Caldarelli, and S. Battiston, Sci. Rep. **3**, 2759 (2013).
[27] M. Bardoscia, S. Battiston, F. Caccioli, and G. Caldarelli, PLoS ONE **10**, e0130406 (2015).
[28] K. Gibson, U.S. stocks hammered after house rejects rescue, https://www.marketwatch.com/story/us-stocks-slide-dow-plunges-777-points-as-bailout-bill-fails-2008929164700.
[29] J. Kwapisz, J. Graph Theory **23**, 405 (1996).
[30] A. Chalkis and V. Fisikopoulos, The R Journal **13**, 642 (2021).
[31] S. Košćak, M. Šikić, H. Štefančić, M. Bešević Vlajo, V. Pribičević, and V. Zlatić, Hub think tank broj 3: Arhitektura mreže dugovanja hrvatskih tvrtki, https://www.hub.hr/hr/hub-think-tank-broj-3-arhitektura-mreze-dugovanja-hrvatskih-tvrtki (text is in Croatian).
[32] I. Barjašić, H. Štefančić, V. Pribičević, and V. Zlatić, Sci. Rep. **11**, 24028 (2021).